SSC17-P1-10

A Comparative Analysis of All-Magnetic Attitude Control Techniques for Nanosatellites Sun Acquisition

Simon Debois, Frederick Viaud
Centre National d'Etudes Spatiales (CNES)
18 Avenue Edouard Belin 31401 Toulouse, France
simon.debois@cnes.fr; frederick.viaud@cnes.fr

ABSTRACT

This work presents 3 candidate strategies for all-magnetic attitude control of a 3U CubeSat using a magnetometer and sun sensors for attitude determination. The study focuses on the sun-acquisition problem and does not treat rate damping (detumbling). The first method is a 'naïve' 3-Axis position control applying torques on each axis depending on the attitude error angle on that axis. This method is well known to yield poor results, but provides a theoretical footing for the rest of the work. The second method takes specificities of actuators and the sun-acquisition problem into account to tailor a better controller. Since the Sun acquisition is a 2-axis positioning problem, this method particularizes the previous one, leaving the pointed axis uncontrolled in rotation. Safeguards are foreseen to avoid velocity build-up on the uncontrolled axis. The last method uses a 2-phases strategy to spin the satellite and provide gyroscopic stiffness before pointing the spun axis towards the sun. The momentum is directed in such a way that if the satellite is perfectly pointed, the momentum is collinear to the target direction. After presenting these 3 strategies, their performances in the simulation environment of CNES are analyzed in terms of pointing accuracy and convergence time.

INTRODUCTION

To fulfil their missions, satellites have to be oriented and stabilized. Whether it is to take a picture of a precise location on the surface of the earth or on the celestial sphere, orient an antenna towards a receiving station, or solar panels towards the sun, a satellite is often required to modify its attitude in space.

When it comes to safety, a major role of the Attitude Control System (ACS) is to ensure that the satellite will always remain under control, whatever happens on board. A dedicated mode of operation is foreseen to face any contingency, and is conveniently called the safe mode. Its main objective is to orient the solar panels towards the sun to insure battery charging.

The safe mode is all the more important for nanosatellites given that the equipment is usually less reliable than conventional space hardware. The spacecraft are thus very likely to spend extended periods of time in that mode following equipment failures.

This study summarizes the work that has been carried out to design and validate an orientation strategy for the safe mode of 3-U CubeSats developed under the supervision of CNES in the context of its education and outreach project JANUS.

All the satellite data used in this work (satellite's inertia, orbital characteristics, etc.) have been taken from EyeSat, which is the reference 3-U cubesat for JANUS, designed and built in CNES. [1, 2]

In the following, the bases of attitude control are recalled as well as of the satellite's dynamics.

The core of the work is then addressed. After a brief review of the objectives and constraints of the safe mode is presented, and a strategy for estimating the angular rates is proposed. 3 candidate attitude control strategies are then presented. For each case, the closed loop dynamic is assessed to determine the stability conditions and compute the controller parameters.

Finally, a comparative analysis of the 3 strategies is carried out based on results obtained in simulations. The selected criteria for this comparison are the batteries' depth of discharge, the convergence time, and the pointing accuracy to a lesser extent.

REFERENCES AND CONVENTIONS

The movement and attitude of a spacecraft is always defined with respect to a reference frame. There can be an infinity of reference frames depending on the satellite and its mission, but it is customary to define at least the following 3

Body reference frame

The body, satellite, or vehicle frame is linked to the satellite platform.

It is usually centered on the spacecraft's center of mass, and its axes correspond to the principal axes of inertia. The chosen BRF is presented in Figure 1.

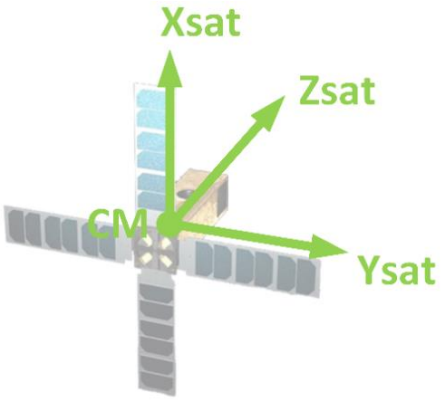

Figure 1: Body reference frame

Local Orbital Frame (LOF)

The origin of the local orbital frame also coincides with the satellite's center of mass, but its axes are not bound to the spacecraft. It is customary to define the Z axis as Nadir pointing (i.e. towards the center of the earth). The X axis is in the direction of the velocity, and the Y axis completes the direct orthogonal system as illustrated in Figure 2.

Inertial Reference Frame (IRF)

The inertial frame is fixed with respect to the stars. When studying Earth-bound satellites, its origin is usually placed at the Earth's center of mass. Its X axis is collinear with the sun-earth direction at the spring equinox (Aries). The Z axis is in the direction of Polaris, and the Y axis completes the direct orthogonal system as illustrated in Figure 2.

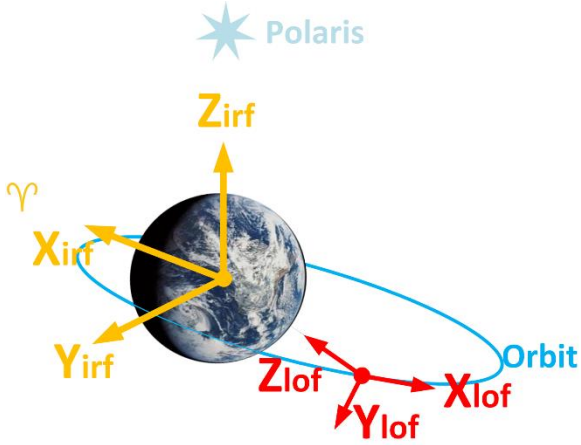

Figure 2: LOF and IRF

Attitude representation

There are 2 different ways to express the attitude. The Euler angles describe 3 successive rotations around 3 axes needed to align the BRF with another reference frame. The axes X, Y, and Z are generally numbered 1, 2, and 3, and the corresponding rotation angles around them are labelled φ, θ, and ψ respectively.

These rotations can be expressed by their rotation matrix as follows:

$$[A_\varphi] = \begin{bmatrix} 1 & 0 & 0 \\ 0 & \cos\varphi & \sin\varphi \\ 0 & -\sin\varphi & \cos\varphi \end{bmatrix}$$
$$[A_\theta] = \begin{bmatrix} \cos\varphi & 0 & -\sin\varphi \\ 0 & 1 & 0 \\ \sin\varphi & 0 & \cos\varphi \end{bmatrix} \quad (1)$$
$$[A_\psi] = \begin{bmatrix} \cos\psi & \sin\psi & 0 \\ -\sin\psi & \cos\psi & 0 \\ 0 & 0 & 1 \end{bmatrix}$$

The order in which the successive rotations are performed is free, which makes 6 possible transformations to get from one frame to another. It is also possible to define transformations in which the first and third rotations are performed about the same axis which makes 6 other possibilities, but they will not be presented here. Each possible transformation is generally referred to by the ordered list of its rotation axes, for example a transformation '1-2-3' means that the first rotation is done around axis 1 (X), and so on. It is interesting to note that, for small angles, the six transformations have the same approximated form which is presented below.

$$[A_{\alpha\beta\gamma}] \cong \begin{bmatrix} 1 & \psi & -\theta \\ -\psi & 1 & \varphi \\ \theta & -\varphi & 1 \end{bmatrix} \quad (2)$$

This representation has the advantage of being intuitive but it necessitates 9 parameters. Moreover, obtaining the angles involves using several trigonometric functions that might cause singularities.

The other way to represent attitude is to use quaternions. Quaternions are 4 dimensional vectors defined as:

$$\boldsymbol{q} = q_4 + \boldsymbol{i}q_1 + \boldsymbol{j}q_2 + \boldsymbol{k}q_3 \quad (3)$$

The conjugate quaternion can also be defined and is expressed as:

$$\boldsymbol{q}^* = q_4 - \boldsymbol{i}q_1 - \boldsymbol{j}q_2 - \boldsymbol{k}q_3 \quad (4)$$

The terms $\boldsymbol{i}$, $\boldsymbol{j}$, and $\boldsymbol{k}$ having the following properties:

$$\begin{aligned} \boldsymbol{i}^2 = \boldsymbol{j}^2 = \boldsymbol{k}^2 = -1 \\ \boldsymbol{ij} = -\boldsymbol{ji} = \boldsymbol{k} \\ \boldsymbol{jk} = -\boldsymbol{kj} = \boldsymbol{i} \\ \boldsymbol{ki} = -\boldsymbol{ik} = \boldsymbol{j} \end{aligned} \quad (5)$$

Their use to express a rotation (and therefore an attitude) is based upon Euler's rotation theorem, which states that any displacement in 3-dimensional space of a rigid body fixed in one point can always be expressed as a single rotation around some axis passing through that fixed point. If this axis is expressed as a unit vector **e**, it can be shown that a rotation of an angle α around that axis can be represented by a quaternion whose parameters are defined as follows:

$$\begin{aligned} q_1 = e_1 \sin\left(\frac{\alpha}{2}\right); q_2 = e_2 \sin\left(\frac{\alpha}{2}\right) \\ q_3 = e_3 \sin\left(\frac{\alpha}{2}\right);\ q_4 = \cos\left(\frac{\alpha}{2}\right) \end{aligned} \quad (6)$$

This allows a very compact and elegant representation and requires only 4 parameters instead of 9 for the Euler angles representation. Furthermore, it is devoid of any singularities.

Quaternions have many interesting properties but a comprehensive presentation is beyond the scope of this work. The interested reader can refer to references on the subject. [3, 4]

SPACECRAFT DYNAMICS

Before designing an attitude control law, it is necessary to understand how a satellite moves in space. The quantity of interest here is the link between the torques applied on the spacecraft and the rate of change of its angular momentum. It can be shown that this relationship can be expressed as follows:

$$\boldsymbol{T}_{tot} = \dot{\boldsymbol{H}}_{irf} = \dot{\boldsymbol{H}}_{brf} + \boldsymbol{\omega} \wedge \boldsymbol{H} \quad (7)$$

With: $\boldsymbol{T}_{tot}$ the sum of all torques applied on the spacecraft [Nm]; $\dot{\boldsymbol{H}}_{irf}$ the derivative of the angular momentum as seen in inertial frame [Nm]; $\dot{\boldsymbol{H}}_{brf}$ the derivative of the angular momentum as seen in body frame [Nm]; $\boldsymbol{\omega}$ the angular velocity of the body frame in the inertial frame [s^{-1}]; $\boldsymbol{H}$ the angular momentum of the spacecraft [Nms]

$\boldsymbol{H}$ being expressed as:

$$\boldsymbol{H} = [I].\boldsymbol{\omega} \quad (8)$$

With $\boldsymbol{I}$ the inertia matrix of the spacecraft:

$$[I] = \begin{bmatrix} I_{xx} & I_{xy} & I_{xz} \\ I_{yx} & I_{yy} & I_{yz} \\ I_{zx} & I_{zy} & I_{zz} \end{bmatrix} [kg.m^2] \quad (9)$$

In the rest of this work, it will be assumed that the inertia matrix is diagonal and constant in time. This hypothesis is known to be valid in the case of 3-U cubesats due to the symmetrical shape of the spacecraft. The inertia matrix is also constant in time as they do not contain any consumables that would be expelled during the mission. It can also be shown that their shape makes the inertia around x and y identical, and the inertia matrix is thus of the form:

$$[I] = \begin{bmatrix} A & 0 & 0 \\ 0 & A & 0 \\ 0 & 0 & C \end{bmatrix} [kg.m^2] \quad (10)$$

For reasons that will be made clear later the spacecraft will not contain any embedded momentum (i.e. inertia wheel) in safe mode, and $\boldsymbol{H}$ is therefore exclusively the angular momentum of the spacecraft itself.

By inserting equation (10) into (8) and then the latter into (7), the following set of equations can be obtained in the body axis frame:

$$\begin{aligned} T_{tot,x} = A\dot{\omega}_x + \omega_y\omega_z(C - A) \\ T_{tot,y} = A\dot{\omega}_y + \omega_x\omega_z(A - C) \\ T_{tot,z} = C\dot{\omega}_z \end{aligned} \quad (11)$$

By stating $\gamma = (C - A)$, one can finally obtain:

$$\begin{aligned} T_{tot,x} = A\dot{\omega}_x + \gamma\omega_y\omega_z \\ T_{tot,y} = A\dot{\omega}_y - \gamma\omega_x\omega_z \\ T_{tot,z} = C\dot{\omega}_z \end{aligned} \quad (12)$$

This fundamental set of equation expresses the attitude dynamic of the satellite, and is the basis upon which an attitude control system can be built.

ANGULAR RATES ESTIMATION

To control the attitude, it is necessary to know it first. For a safe mode the task is simplified by the fact that the objective is to point towards the sun, and that it is assumed that the satellite is fitted with sun sensors. The setpoint is therefore directly measurable in body frame. As in safe mode one only needs to align 2 vectors, the sun direction vector is sufficient to insure proper pointing. Considering the sun as being inertial, measuring its position gives information about the position of the satellite in inertial frame.

Provided that the sun sensors give the unit sun direction vector:

$$\boldsymbol{s_{brf}} = \left[S_{x,brf}\ S_{y,brf}\ S_{z,brf}\right]^T \quad (13)$$

The positioning error is determined as the difference between the vector normal to the solar panels $(-\boldsymbol{z_{brf}})$ and the direction of the sun in body frame $\mathbf{s_{brf}}$.

The axis of rotation **R** around which the satellite must move is defined as the cross product:

$$\boldsymbol{R_{brf}} = (-\boldsymbol{z_{brf}}) \wedge \boldsymbol{s_{brf}} \quad (14)$$

The error angle α can either be obtained from the cross product or from the scalar product:

$$\begin{aligned} \sin\alpha &= \left\|\boldsymbol{R_{brf}}\right\| \\ \cos\alpha &= (-\boldsymbol{z_{brf}} \bullet \boldsymbol{s_{brf}}) \end{aligned} \quad (15)$$

It is preferable to use the first expression, as it reduces to $\alpha = \left\|\boldsymbol{R_{brf}}\right\|$ for small error angles.

In addition to the attitude, angular rates must also be measured. The estimation strategy is here based on a combination between the magnetic and solar measurements, or magnetic measurements alone while the satellite is in eclipse.

The strategy has been developed for the Myriade family of satellites and can be summarized as follows: [5]

Let **u** be a unit vector. Its derivative in inertial frame can be expressed as:

$$\frac{d\boldsymbol{u}}{dt}_{IRF} = \frac{d\boldsymbol{u}}{dt}_{Brf} + \omega \wedge \boldsymbol{u} \quad (16)$$

With ω the angular speed of the BRF with respect to the IRF.

The estimation principle supposes that the inertial velocity of **u** is negligible with respect to the satellite angular rate, which means:

$$\frac{d\boldsymbol{u}}{dt}_{IRF} = 0 \quad (17)$$

Equation (16) can therefore be re-written as:

$$\frac{d\boldsymbol{u}}{dt}_{Brf} + \omega \wedge \boldsymbol{u} = 0 \quad (18)$$

This relationship shows that only the 2 components of ω that are perpendicular to **u** can be estimated. This leads to the estimated angular rate $\widehat{\omega}$

$$\widehat{\omega} = \frac{\dot{\boldsymbol{u}} \wedge \boldsymbol{u}}{\|\boldsymbol{u}\|} = \dot{\boldsymbol{u}} \wedge \boldsymbol{u} \quad (19)$$

From a signal processing point of view, the derivative of **u** can be computed as:

$$\dot{\boldsymbol{u}} = \frac{\boldsymbol{u_k} - \boldsymbol{u_{k-1}}}{\Delta T} \quad (20)$$

ΔT being the sampling period of the ACS, and $\boldsymbol{u_k}$ and $\boldsymbol{u_{k-1}}$ the measurements at time k and k-1 respectively.

Inserting equation (20) into (19) finally gives the angular rates estimates as a function of the measurements:

$$\widehat{\omega} = \frac{\boldsymbol{u}_k \wedge \boldsymbol{u}_{k-1}}{\Delta T} \quad (21)$$

This technique can be applied to the measurements of the magnetic field and solar direction. The 2 measurements thus provide 2 partial estimates:

$$\begin{aligned} \widehat{\boldsymbol{\omega}}_k^B &= \frac{\boldsymbol{b}_k \wedge \boldsymbol{b}_{k-1}}{\Delta T} \\ \widehat{\boldsymbol{\omega}}_k^S &= \frac{\boldsymbol{s}_k \wedge \boldsymbol{s}_{k-1}}{\Delta T} \end{aligned} \quad (22)$$

With $\boldsymbol{b}$ the direction of the magnetic field $\boldsymbol{B}$.

In the case of the magnetic field, the hypothesis stating that the vector is inertial is not met, as its direction will vary all along the orbit. But this variation can be considered as negligible as far as angular rates are concerned. Indeed, the field rotates twice during an orbit, which for a 700km SSO circular orbit represents a period of around 3000s, and an angular rate of only 0.0021 rad/s.

As each vector will provide 2 components of the angular rate, and that they are never aligned on the selected orbit, the combination of the 2 estimates will provide a 3-axis estimation of the angular rate.

These can be merged together in the following manner: During detumbling, the sun direction measurement is considered as less precise and is exploited only on the axis which is not covered by the magnetic field measurement:

$$\widehat{\boldsymbol{\omega}}^{S+B} = \widehat{\boldsymbol{\omega}}^B + (\widehat{\boldsymbol{\omega}}^S \bullet \boldsymbol{b})\boldsymbol{b} \quad (23)$$

During sun acquisition on the other hand, the sun direction measurement is considered as more precise and is fully exploited. The magnetic measurement completes the estimate:

$$\widehat{\boldsymbol{\omega}}^{S+B} = \widehat{\boldsymbol{\omega}}^{S} + (\widehat{\boldsymbol{\omega}}^{B} \bullet \boldsymbol{s})\boldsymbol{s} \quad (24)$$

In both cases, the complete estimate $\widehat{\boldsymbol{\omega}}^{S+B}$ is composed of the partial estimate deemed the more reliable, and from the component of the less reliable estimate that is collinear to the reference vector.

To improve the quality of the estimation, partial estimates can be filtered using a first order linear filter whose characteristics depend upon the noise pattern of each measurement.

CONTROL SYSTEM SPECIFICATIONS

The aim of the safe mode is ultimately to insure battery charging. The ACS must reach and maintain an attitude in which the solar panels are pointed towards the sun with a reasonable angle. It usually consists of 2 phases: Firstly, the angular rates must be damped in order to stabilize the satellite. Then, the solar panels must be pointed towards the sun to insure the energy supply and thermal equilibrium. The first phase is generally known as *Detumbling*, while the second is called *sun acquisition* for obvious reasons.

Detumbling is generally based on a very simple magnetic control law called 'b-dot'. This law is well mastered and has already been implemented and optimized in the context of Eyesat and a number of other cubesats all around the world. It will therefore be presented, but not be studied in detail in this work. The design effort will thus be exclusively focused on the sun-acquisition phase.

It can be considered that the energy received by a solar panel is proportional to the cosine of the angle α_{sol} between its normal vector (**-$\mathbf{Z_{sat}}$** for Robusta) and the direction of the sun **S**. Considering then that when the panels are perfectly perpendicular to the direction of the sun they produce their maximum power P_{max}**,** the available input power P_a can be expressed as:

$$\begin{aligned} P_a &= P_{max}.(-\boldsymbol{Z_{sat}} \bullet \boldsymbol{S}) \\ &= P_{max}.\cos\alpha_{sol} \end{aligned} \quad (25)$$

To insure a positive energy balance, it is imperative to maintain this available power higher than the consumed power P_c as far as possible. After convergence it is absolutely necessary that $P_a > P_c$, and the pointing requirement can thus be expressed as:

$$\alpha_{sol} < \cos^{-1}\left(\frac{P_c}{P_{max}}\right) \quad (26)$$

For 3U cubesats having a 'flower' configuration with 4 solar panels, P_{max} is approximately 24 Watts.

Concerning the consumption on the other hand, no precise information being available, estimation based on the rated power of Eyesat's magnetorquer, magnetometer, and on-board computer led to an approximated power consumption of around 12 Watts while exposed to the sun, and 4 while in eclipse. The consumption is lower in eclipse due to the fact that the sun being by definition invisible, sun-acquisition is impossible, and no attitude control is performed.

This information finally allows obtaining a clear numeric target for the pointing requirement after convergence:

$$\begin{aligned} \alpha_{sol} &< \cos^{-1}\left(\frac{12}{24}\right) \\ &< 60\ [°] \end{aligned} \quad (27)$$

For safety reasons however, this requirement will be tighten to 30°. In addition to this, the convergence time is constrained by the battery capacity C_{bat} and its maximum allowable depth of discharge DoD_{max}.

Considering that the satellite does not receive any energy as long as the attitude has not converged, the maximum allowable convergence time T_{conv} can be expressed as:

$$T_{conv} < \frac{C_{bat}.DoD_{max}}{P_c}\ [h] \quad (28)$$

Considering a battery capacity worth 47.6 Watt.h, and that the battery must never be discharged more than 60% of this value at the end of the first acquisition, this gives a total of 28.56 Watt.h available to slow down the satellite and reach the required attitude.

$$\begin{aligned} T_{conv} &< \frac{47.6 * 0{,}6}{10}\ [h] \\ T_{conv} &< 10281\ [s] \end{aligned} \quad (29)$$

It has to be reminded however that this computation considers no energy input during the whole process of convergence, which will not be true, especially considering the fact that an angle between the solar panels' normal vector and the sun director of 60° is already sufficient to cover the energy needs. This requirement must therefore be considered with caution.

Finally, a last requirement must be set concerning the hardware to be used in safe mode. As already mentioned the ultimate fallback mode must only depend upon the most reliable sensors and actuators. If in conventional satellites reaction wheels can be regarded as such, it is not yet the case for nanosatellites. For this reason, it has been decided that the Safe mode should only use the magnetorquers for actuation.

Concerning attitude determination, the magnetometer and the sun sensors being both very reliable, they can all be used in safe mode.

CONTROL WITHOUT INDUCED KINETIC MOMENTUM

Control Strategy

Control without kinetic momentum basically applies torques on each axis depending on the attitude error angle on that axis. Such a control law could be expressed as:

$$\boldsymbol{T} = \boldsymbol{K}((-\boldsymbol{z_{brf}}) \wedge \boldsymbol{s_{brf}}) \tag{30}$$

With: **T** the control torque vector [Nm]; **K** the control gain vector.

This is a simple proportional law, but any other classical control technique such as PID could be applied.

When on the other hand the satellite possesses an on-board kinetic momentum, it responds differently to applied torques, and the previous technique cannot be used anymore.

Controller synthesis

A simple control law based on the pointing error can be obtained using a classical Proportional derivative controller. The derivative term is added to avoid oscillations that would certainly occur with a proportional gain alone as the system is an undamped second order. For a pointing error α_e on a given axis, the control torque is thus of the form:

$$T_c = K_p\alpha_e + K_d\dot{\alpha}_e \tag{31}$$

The pointing error being expressed $\alpha_e = \alpha_{sp} - \alpha$ with sp standing for setpoint, equation (30) can be expanded as:

$$T_c = K_p\alpha_{sp} - K_p\alpha + K_d\dot{\alpha}_{sp} - K_d\dot{\alpha} \tag{32}$$

Then, knowing that the setpoint will never vary, the final expression of the control torque can finally be obtained:

$$T_c = K_p(\alpha_{sp} - K_p\alpha) - K_d\dot{\alpha} \tag{33}$$

For sun acquisition, the pointing error around Z has no meaning since axes X and Y can point in any direction without impacting the power supply. The aim of the controller will therefore simply be to ensure that the satellite does not rotate around Z.

As this represent controlling a first order system, a simple gain can be used.

These expressions can be inserted in the equations of dynamics (12) that have been reproduced hereunder to determine the closed loop dynamics of the satellite.

$$\begin{aligned} T_{tot,x} &= A\dot{\omega}_x + \gamma\omega_y\omega_z \\ T_{tot,y} &= A\dot{\omega}_y - \gamma\omega_x\omega_z \\ T_{tot,z} &= C\dot{\omega}_z \end{aligned} \tag{34}$$

For the sake of clarity, Euler angles will be used in this development, and it will be assumed that the small angles hypothesis is valid. In that case the following relationships hold:

$$\begin{aligned} \omega_x &= \dot{\varphi} \\ \omega_y &= \dot{\theta} \end{aligned} \tag{35}$$

Furthermore, as the sun acquisition phase follows detumbling, it can be assumed that ω_z is small and might only vary slowly with respect to the other terms, and can therefore be considered as constant. The coupling term γ being constant as well, let us define a new constant $\Gamma = \gamma\omega_z$.The dynamics equations can now be re-written:

$$\begin{aligned} T_{tot,x} &= A\dot{\omega}_x + \Gamma\omega_y \\ T_{tot,y} &= A\dot{\omega}_y - \Gamma\omega_x \\ T_{tot,z} &= C\dot{\omega}_z \end{aligned} \tag{36}$$

Inserting equations (34) and (35) into (36) finally leads to the expression of the closed loop dynamics:

$$\begin{aligned} -K_p\varphi - K_d\dot{\varphi} &= A\ddot{\varphi} + \Gamma\dot{\theta} \\ -K_p\theta - K_d\dot{\theta} &= A\ddot{\theta} - \Gamma\dot{\varphi} \\ -K_s\omega_z &= C\dot{\omega}_z \end{aligned} \tag{37}$$

Solving the last equation shows that ω_z is of the form:

$$\omega_z(t) = e^{-\frac{K_s}{C}t} \tag{38}$$

Which will converge to zero as long as the gain K_s is positive.

Since the dynamics of the third axis is supposed to be very slow and is unaffected by that of the other axes they can be studied separately.

The 2 first equations of (37) can be rearranged as:

$$\begin{aligned}\ddot{\varphi} &= -\frac{K_p}{A}\varphi - \frac{K_d}{A}\dot{\varphi} - \frac{\Gamma}{\mathrm{A}}\dot{\theta} \\ \ddot{\theta} &= -\frac{K_p}{A}\theta - \frac{K_d}{A}\dot{\theta} + \frac{\Gamma}{\mathrm{A}}\dot{\varphi}\end{aligned} \tag{39}$$

This system can then be expressed in matrix form:

$$\begin{bmatrix}\dot{\varphi}\\ \dot{\theta}\\ \ddot{\varphi}\\ \ddot{\theta}\end{bmatrix} = \begin{bmatrix} 0 & 0 & 1 & 0 \\ 0 & 0 & 0 & 1 \\ -\frac{K_p}{A} & 0 & -\frac{K_d}{A} & -\frac{\Gamma}{\mathrm{A}} \\ 0 & -\frac{K_p}{A} & \frac{\Gamma}{\mathrm{A}} & -\frac{K_d}{A}\end{bmatrix}\begin{bmatrix}\varphi\\ \theta\\ \dot{\varphi}\\ \dot{\theta}\end{bmatrix} \tag{40}$$

It can be shown that the eigenvalues of this matrix are the roots of the equation:

$$\left[\lambda\left(\frac{K_d}{A}+\lambda\right)+\left(\frac{K_p}{A}\right)\right]^2 + \left(\frac{\lambda\Gamma}{A}\right)^2 = 0 \tag{41}$$

Which can be further transformed as:

$$\lambda\left(\frac{K_d}{A}+\lambda\right)+\left(\frac{K_p}{A}\right) = j\frac{\lambda\Gamma}{A} \tag{42}$$

Then, expanding the left-hand side finally leads to:

$$\lambda^2 + \left(\frac{K_d}{A} - j\frac{\Gamma}{A}\right)\lambda + \frac{K_p}{A} = 0 \tag{43}$$

It can be noticed that if the angular velocity around Z is zero the Γ term vanishes, and the equation reverts to the characteristic polynomial of a second order system.

In the general case, the roots of the equation are of the form:

$$\lambda_0 = \frac{-\left(\frac{K_d}{A} - j\frac{\Gamma}{A}\right) \pm \sqrt{\left(\frac{K_d}{A} - j\frac{\Gamma}{A}\right)^2 - \frac{4K_p}{A}}}{2} \tag{44}$$

Solving this equation involves taking the root of a complex number, which in this case cannot be done analytically. It is nevertheless possible to detect a trend concerning the impact of the spin. If Γ is small, it has already been seen that the roots revert to those of a simple second order system.

If on the other hand Γ is big with respect to the term $\frac{K_d}{A}$, the latter can be neglected, and the roots become:

$$\lambda_{0,\Gamma\gg} = \frac{j\frac{\Gamma}{A} \pm \sqrt{\left(\frac{\Gamma}{A}\right)^2 - \frac{4K_p}{A}}}{2} \tag{45}$$

In that case, 2 solutions are possible:

- $\left(\frac{\Gamma}{A}\right)^2 > \frac{4K_p}{A}$

In that case the term under the square root is real, and 1 of the eigenvalues has a positive real part. This situation therefore leads to instability.

- $\left(\frac{\Gamma}{A}\right)^2 \leq \frac{4K_p}{A}$

In that case the term under the square root is complex or zero and the eigenvalues are purely complex. The system is thus undamped, but theoretically (critically) stable.

All this shows that the spin around the Z-axis clearly has a negative impact on the control system. It is therefore very important to have $K_p \geq \frac{\Gamma^2}{4A}$. As it is not possible to make the gain arbitrarily large due to actuator saturation, the spin must be reduced as much as possible.

2 solutions have been considered in order to control the spacecraft using the strategy presented above. The first option is trying to control the dynamics of the Z-axis in order to maintain its spin as low as possible, and designing the controllers of the 2 other axes considering a zero value of spin.

The second option is to consider that as the sun-acquisition phase is performed after detumbling, the angular rates around all axes are very small. As the disturbances are also small, the spin around z is unlikely to increase very quickly. It is thus possible to consider controlling only the 2 other axes while leaving Z uncontrolled. In order to avoid instability, the spin around Z must nevertheless be monitored permanently, and if the spin were to become too important, the ACS would trigger a new detumbling phase.

The simplest implementation of this method is to monitor the norm of the angular rate vector, and giving back total control to the detumbling controller if the spin becomes too important. However, this hard switch would create discontinuities that could bring instability.

Smoother transition between the 2 laws can be obtained using a kind of fuzzy logic controller that will continuously monitor the norm of the angular rate vector, and adjust the influence of the 2 laws on the commanded torque. That logic is illustrated in Figure 3.

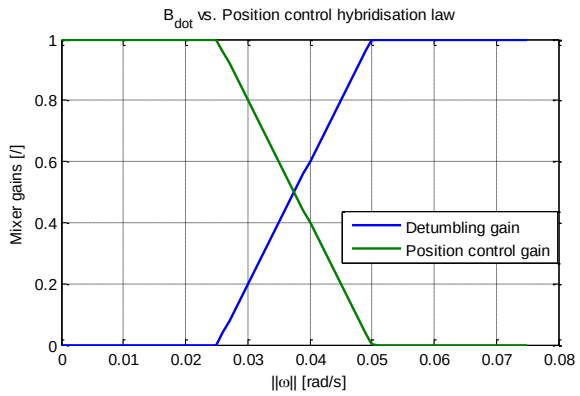

Figure 3: Fuzzy logic hybridization law

In that precise case, one can see that when the norm of the angular rate vector $\|\omega\|$ is lower than 0.025 rad/s, the detumbling controller is disconnected (zero gain) and the satellite is completely controlled by the position controller. If the norm is higher than 0.05 rad/s on the other hand, it is the position controller that is disconnected, and the satellite is fully in detumbling.

As it stays in detumbling, the satellite will slow down and $\|\omega\|$ will decrease, bringing the 'cursor' on the left of the graph. The less it rotates, the more it becomes controllable and the more the position controller will affect its dynamics.

The 2 main parameters of this mechanism for the present application are the value of $\|\omega\|$ for which the Position control gain begins to decrease, and the width of the transition region. Indeed, if the position control law is allowed to act for excessive values of spin, the satellite will become unstable. If the transition region is too broad, the satellite might be trapped in a region where no law supersedes the other, and if it is too tight the situation will revert to that of a hard switch and possibly create instability.

Let T be the threshold on the value of $\|\omega\|$ for which the Position control gain begins to decrease, and L the length of the transition region. The Detumbling gain G_{dtb} variation in that area can be expressed as:

$$G_{dtb} = \frac{1}{L}(\|\omega\| - T) \tag{46}$$

By bounding this equation between 0 and 1, the blue curve of Figure 3 is obtained.

The evolution of the position control law gain G_{pc} is then computed as:

$$G_{pc} = 1 - G_{dtb} \tag{47}$$

In both strategies, the controllers of the X and Y axes are designed considering the spin around Z is zero. The difference between the 2 techniques is that in the first case the gain Ks of equation (38) is non-zero, whereas in the second strategy it is.

CONTROL WITH INDUCED KINETIC MOMENTUM

Control Strategy

Kinetic momentum can be applied to provide gyroscopic stability to the spacecraft, but in return it resists the control torques. The aim of the positioning control law is therefore not to fight against the momentum, but to use it to modify the attitude. Unlike in the previous technique, the toque must here be directed in the desired direction of motion to increase the component of the momentum in that direction and tilt the satellite.

The momentum is directed in such a way that if the satellite is perfectly pointed, the momentum is collinear to the target direction. In conventional satellite it can be provided by inertia wheels. In this study however the use of wheels is forbidden in safe mode and it is the satellite itself that needs to be spun in order to provide the momentum.

3-U cubesats allow to implement this strategy easily, as the dynamics of the axis that needs to be spun (Z) is decoupled from the others, as has been shown in the previous section dedicated to spacecraft dynamics.

The strategy in that case is therefore to spin the satellite about its Z axis, and then to orient the resulting kinetic momentum $\boldsymbol{H}$ in the desired direction. The torques needed to achieve this goal must follow the relationship:

$$\boldsymbol{T} = \boldsymbol{K}(\boldsymbol{H} \wedge (\boldsymbol{s} \wedge \boldsymbol{H})) \tag{48}$$

Knowing that this law will be applied in the context of magnetic control, equation (47) can be modified to take into account the fact that the control torque must be orthogonal to the Earth's magnetic field **B**.

First of all, let's develop the double cross product:

$$\begin{aligned} \boldsymbol{H} \wedge (\boldsymbol{s} \wedge \boldsymbol{H}) &= \boldsymbol{s}(\boldsymbol{H} \bullet \boldsymbol{H}) - \boldsymbol{H}(\boldsymbol{H} \bullet \boldsymbol{s}) \\ &= \|\boldsymbol{H}\|^2 \boldsymbol{s} - \boldsymbol{H}(\boldsymbol{H} \bullet \boldsymbol{s}) \end{aligned} \tag{49}$$

The torque must be orthogonal to **B**, but as this law concerns only the reorientation there should be no torque acting in the direction of the momentum **H** either. These constraints can be guaranteed by projecting the torque vector computed previously on the vector $(\boldsymbol{b} \wedge \boldsymbol{h})$.

$$\begin{aligned}\boldsymbol{T_a} &= [\boldsymbol{T_d} \bullet (\boldsymbol{b} \wedge \boldsymbol{h})](\boldsymbol{b} \wedge \boldsymbol{h}) \\ &= [\|\boldsymbol{H}\|^2(\boldsymbol{b} \wedge \boldsymbol{h}) \bullet \boldsymbol{s} - (\boldsymbol{H} \bullet \boldsymbol{s})(\boldsymbol{b} \wedge \boldsymbol{h}) \\ &\qquad \bullet \boldsymbol{H}](\boldsymbol{b} \wedge \boldsymbol{h})\end{aligned} \tag{50}$$

With: $\boldsymbol{T_a}$ the actual torque that can be produced by the magnetic actuators. [Nm]; $\boldsymbol{T_d}$ the desired control torque [Nm].

In the last equation, in is interesting to note that:

$$(\boldsymbol{b} \wedge \boldsymbol{h}) \bullet \boldsymbol{H} = \boldsymbol{b} \bullet (\boldsymbol{h} \wedge \boldsymbol{H}) = 0 \tag{51}$$

And equation (50) can therefore be simplified as:

$$\mathrm{T_a} = [\|\boldsymbol{H}\|^2(\boldsymbol{b} \wedge \boldsymbol{h}) \bullet \boldsymbol{s}](\boldsymbol{b} \wedge \boldsymbol{h}) \tag{52}$$

Contrarily to what has been done until now, the aim here is not to prevent the satellite from spinning, but to induce that movement.

This technique requires 2 separate controllers. A first control law will produce and maintain the requested kinetic momentum properly oriented in the satellite frame and with the good magnitude, and a second will orient this momentum in inertial space.

Spin Controller Synthesis

As already mentioned, the aim of the spin controller is to control the kinetic momentum of the spacecraft. This amount to controlling a first order system and the use of a derivative action is not required. A simple proportional law can thus be used, and the control torque can be expressed as:

$$\boldsymbol{T_{spin}} = K_s(\boldsymbol{H_{sp}} - \boldsymbol{H_m}) \tag{53}$$

Hsp and **Hm** being respectively the kinetic momentum setpoint and actual vectors. [6]

The inertia matrix being diagonal, the components of the torques are simply:

$$\begin{aligned}T_{spin,x} &= K_s A(\omega_{x,sp} - \omega_x) \\ T_{spin,y} &= K_s A(\omega_{y,sp} - \omega_y) \\ T_{spin,z} &= K_s C(\omega_{z,sp} - \omega_z)\end{aligned} \tag{54}$$

Inserting these torques in the dynamics equations, one obtains:

$$\begin{aligned}K_s A(\omega_{x,sp} - \omega_x) &= A\dot{\omega}_x + \gamma\omega_y\omega_z \\ K_s A(\omega_{y,sp} - \omega_y) &= A\dot{\omega}_y - \gamma\omega_x\omega_z \\ K_s C(\omega_{z,sp} - \omega_z) &= C\dot{\omega}_z\end{aligned} \tag{55}$$

In order to develop these equations any further, some simplifications are necessary. First of all, only the particular case of the safe mode will be considered, and the setpoint on x and y will be to zero. Secondly, ω_z will be considered as slowly varying, this time around its setpoint value, which implies:

$$\begin{aligned}&\omega_z(t) = \Omega_{z,sp} + \epsilon_z(t)\ ;\ (\epsilon_z \ll \Omega_z) \\ &\dot{\omega}_z(t) = \dot{\epsilon}_z(t)\end{aligned} \tag{56}$$

This allows re-writing the equation (55) as:

$$\begin{aligned}\dot{\omega}_x &= -K_s\omega_x - \frac{\gamma}{\mathrm{A}}\Omega_z\omega_y \\ \dot{\omega}_y &= -K_s\omega_y + \frac{\gamma}{\mathrm{A}}\Omega_z\omega_x \\ \dot{\epsilon}_z &= -K_s\epsilon_z\end{aligned} \tag{57}$$

This set of equation now being linear, it can be expressed in state-space form:

$$\begin{bmatrix}\dot{\omega}_x \\ \dot{\omega}_y \\ \dot{\epsilon}_z\end{bmatrix} = \begin{bmatrix}-K_s & -\frac{\gamma}{\mathrm{A}}\Omega_z & 0 \\ \frac{\gamma}{\mathrm{A}}\Omega_z & -K_s & 0 \\ 0 & 0 & -K_s\end{bmatrix}\begin{bmatrix}\omega_x \\ \omega_y \\ \epsilon_z\end{bmatrix} \tag{58}$$

Whose characteristic polynomial can be found:

$$-(K_s + \lambda)\left[(K_s + \lambda)^2 + \left(\frac{\gamma}{\mathrm{A}}\Omega\right)^2\right] = 0 \tag{59}$$

Polynomial from which the eigenvalues can be obtained and are worth:

$$\begin{aligned}\lambda_1 &= -K_s \\ \lambda_{2,3} &= -K_s \pm j\frac{\gamma\Omega_z}{A}\end{aligned} \tag{60}$$

This result is very interesting for various reasons. First of all, it shows that the spin controller is stable provided that the gain is positive. Secondly, the eigenvalues have a very clear physical significance, and can easily be linked to the dynamics of the satellite.

The first eigenvalue is real and is not impacted by the spin around Z because it corresponds to the dynamics around that axis, which is decoupled from the others. The 2 other eigenvalues correspond to the 2 other axis and are impacted by the spin. The kinetic momentum around these 2 axes will tend to oscillate due to the spin and the coupling term, and this appears here in the form of the complex term of the eigenvalue.

The choice of the gain is not critical as the system is stable anyway. However, it is better to take a gain that is higher than the complex part of the root, as it will decrease the amplitude of the oscillations and the settling time.

Position Controller Synthesis

The aim of the controller is not here to modify the position of the satellite directly, but of the direction of the kinetic momentum. It was shown earlier in this work that this control requires torques following the command law:

$$T_{pos} = K_a \|\boldsymbol{H}\|^2((\boldsymbol{b} \wedge -\boldsymbol{z}) \bullet \mathbf{s})(\mathbf{b} \wedge -\mathbf{z}) \tag{61}$$

This expression can be expanded to express the components along x and y:

$$\begin{aligned} T_{pos,x} &= K_a \|\boldsymbol{H}\|^2(s_x b_y^2 - s_y b_x b_y) \\ T_{pos,y} &= K_a \|\boldsymbol{H}\|^2(s_y b_x^2 - s_x b_x b_y) \end{aligned} \tag{62}$$

Let's simplify these equations by posing:

$$\begin{aligned} \beta_y &= K_a \|\boldsymbol{H}\|^2 b_y^2 \\ \beta_{xy} &= K_a \|\boldsymbol{H}\|^2 b_x b_y \\ \beta_x &= K_a \|\boldsymbol{H}\|^2 b_x^2 \end{aligned} \tag{63}$$

The expressions of the torques thus become:

$$\begin{aligned} T_{pos,x} &= \beta_y s_x - \beta_{xy} s_y \\ T_{pos,y} &= \beta_x s_y - \beta_{xy} s_x \end{aligned} \tag{64}$$

As the aim is to align the sun direction vector with –z, the components s_x and s_y represent error signals that must be zeroed. Therefore, it can be considered that:

$$\begin{aligned} s_x &\simeq \varphi_e = -\varphi \\ s_y &\simeq \theta_e = -\theta \end{aligned} \tag{65}$$

And the torques can finally be linked to the attitude angles:

$$\begin{aligned} T_{pos,x} &= \beta_{xy}\theta - \beta_y \varphi \\ T_{pos,y} &= \beta_{xy}\varphi - \beta_x \theta \end{aligned} \tag{66}$$

Once again, the expression of the control torques can be inserted in the dynamics equations. As the position controller is only concerned by axes x and y, there are only 2 equations to study. Moreover, as the angular velocity around z is supposed to be maintained constant by the spin controller, it will be considered as such.

$$\begin{aligned} \beta_{xy}\theta - \beta_y \varphi &= A\ddot{\varphi} + \gamma\omega_z \dot{\theta} \\ \beta_{xy}\varphi - \beta_x \theta &= A\ddot{\theta} - \gamma\omega_z \dot{\varphi} \end{aligned} \tag{67}$$

Posing $\Gamma = \gamma\omega_z$ and rearranging the terms to isolate the second derivatives, the equations finally become:

$$\begin{aligned} \ddot{\varphi} &= \frac{\beta_{xy}}{A}\theta - \frac{\beta_y}{A}\varphi - \frac{\Gamma}{A}\dot{\theta} \\ \ddot{\theta} &= \frac{\beta_{xy}}{A}\varphi - \frac{\beta_x}{A}\theta + \frac{\Gamma}{A}\dot{\varphi} \end{aligned} \tag{68}$$

Putting these equations in the form of a matrix, one obtains the following state-space representation:

$$\begin{bmatrix} \dot{\varphi} \\ \dot{\theta} \\ \ddot{\varphi} \\ \ddot{\theta} \end{bmatrix} = \begin{bmatrix} 0 & 0 & 1 & 0 \\ 0 & 0 & 0 & 1 \\ -\frac{\beta_y}{A} & \frac{\beta_{xy}}{A} & 0 & -\frac{\Gamma}{A} \\ \frac{\beta_{xy}}{A} & -\frac{\beta_x}{A} & \frac{\Gamma}{A} & 0 \end{bmatrix} \begin{bmatrix} \varphi \\ \theta \\ \dot{\varphi} \\ \dot{\theta} \end{bmatrix} \tag{69}$$

One can then compute its characteristic polynomial:

$$\lambda^2\left(\lambda^2 + \left(\frac{\Gamma}{A}\right)^2 + \frac{\beta_x + \beta_y}{A}\right) = 0 \tag{70}$$

And the eigenvalues are finally obtained:

$$\begin{aligned} \lambda_{1,2} &= 0 \\ \lambda_{3,4} &= \pm j\sqrt{\left(\frac{\Gamma}{A}\right)^2 + \frac{\beta_x + \beta_y}{A}} \end{aligned} \tag{71}$$

Replacing β_x and β_y by their expressions gives for the last 2 eigenvalues:

$$\lambda_{3,4} = \pm j\sqrt{\left(\frac{\Gamma}{A}\right)^2 + K_a\frac{\|\boldsymbol{H}\|^2(b_x^2 + b_y^2)}{A}} \tag{72}$$

The eigenvalues are purely imaginary, which is logical if one thinks that any torque applied on the x and y axes will inevitably cause the satellite to oscillate due to the momentum on z.

From a control point of view, the eigenvalues show that to have any influence on the movement of the satellite, one must have:

$$K_a \frac{\|\boldsymbol{H}\|^2(b_x^2 + b_y^2)}{A} \geq \left(\frac{\Gamma}{A}\right)^2 \quad (73)$$

In parallel to this requirement, it must be insured that the eigenvalue is not too important as it would make the system oscillate much quicker, and possibly harder to control.

Kinetic momentum computation

In the 2 preceding sections, one could see the eigenvalues of the system are balanced between the gains and the value of the angular momentum. In order to choose the gains properly, it is therefore necessary to determine first the desired kinetic momentum around axis Z.

The bigger the momentum, the steadier the satellite. However, an important momentum might make it harder to control the satellite. Furthermore, it might create problems which are not linked to the satellite's dynamics, but with the control system. Indeed, in order to provide the requested torques, the controller must measure the ambient magnetic field, and adapt the momentum created by the coils. However, the coils themselves disturb significantly the field around the magnetometer, and they must therefore be shut down in order to perform a valid measurement of the earth's magnetic field.

To make sure the measurements are properly executed, a technique called *time sharing* is put in place. This technique consists in allowing different time slots for the different actions that have to be performed by the controller, namely measuring, and then controlling.

For a flight software period T_{fs} of 1 second, 200 milliseconds will be allotted to the magnetic field measurement and the computation of the command torques (T_{mes}). The rest will be left for the actuation (T_{act}), as illustrated in Figure 4.

Assuming an instantaneous measurement at the beginning of the flight software period, the magnetic field is considered constant in satellite frame during the next second. It is not the case however since the satellite is spinning at ω_{spin}, and an error angle α_e will appear between the measured and real magnetic field vector. At the end of the flight software period, this error will amount to:

$$\alpha_e = \omega_{spin} T_{fs} \quad (74)$$

To limit this error, the spin will be chosen so that α_e is similar to the precision of the magnetometer. The latter being in the order of magnitude of 2° for cubesat magnetometers, the maximum value for ω_{spin} can be obtained:

$$\omega_{spin} \leq 35.10^{-3}\ rad/s \quad (75)$$

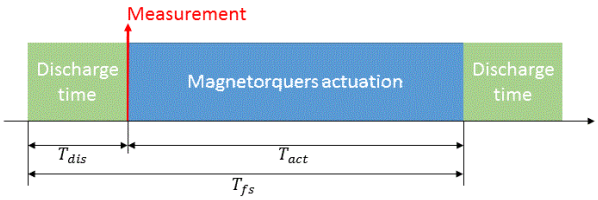

Figure 4: Time sharing chronogram

SIMULATIONS AND RESULTS

All the results presented below were obtained with 25000s simulations on a 10h30 orbit with non-zero initial conditions on angular rates (0.2 rad/s on each axis). The characteristics of the satellite were those of EyeSat.

These simulations were performed in the simulation environment developed by the AOCS department of CNES running on Matlab and Simulink.

The most important criteria used to evaluate the performance of each strategy is the battery's depth of discharge, which is the most important quantity to monitor in safe mode.

Another important criterion is the convergence time. In the following results, it has been defined as the time between the activation of the acquisition phase and the moment at which the battery reaches its maximum DoD.

The best convergence time and minimum depth of discharge where obtained for the 3-axis position controller with kinetic momentum. A sweep on the values of Ka and Ks was conducted for values of spin ranging from 0.01 to 0.035.

The results obtained for a spin of 0.02 and 0.03 are presented in Figure 5 and Figure 6 respectively. These results are highly dependent on the inertia matrix of the spacecraft, as it was shown in the previous theoretical analysis, and cannot be generalized.

For Eyesat, a minimum theoretical value for Ka of 8.4 had been found for an angular rate of 0.035, and it can be observed that a 'valley' of minima does exist for the values of Ka that are close to that condition. The values of Ks also seem to be appropriate. Indeed, the results are good which shows that the kinetic momentum is properly managed, and yet the variations of Ks do not impact strongly the result in the interesting region. This shows that the position controller is not hugely impacted by the spin controller, which is exactly what was expected.

Concerning the choice of the kinetic momentum, the best values of both convergence time and DoD are obtained for the most important angular rate (0.03). Moreover, the width of the 'valley' is much larger in that case, which leaves more margins for uncertainties.

The best results for both angular rates are presented in Table 1. For the smallest rate value, the best convergence time and DoD are not reached for the same settings, which is why there are 2 gain values for Ka.

Table 1: best results for convergence time and DOD

Parameter	$\omega_z = 0.02$ $[rad/s]$	$\omega_z = 0.03$ $[rad/s]$
Ka (Tconv/DOD) [/]	6.84/10.53	12.37
Ks [/]	0.001-0.02	0.001-0.02
Convergence time [s]	4560	3900
Maximum DOD (%)	17.3	16.7

The convergence time presented in Table 1 includes the detumbling phase. The maximum depth of discharge remains well below 30% in both cases as requested.

As the 2-axis controller with kinetic momentum monitoring is a particular case of the 3-axis controller without kinetic momentum, the results for both controllers could be obtained from the same simulation campaign, and are presented in Figure 7and Figure 8.

This campaign swept the values of both gains (Kp/Kd) on large intervals which allowed bringing to light an interesting fact.

A first campaign had been carried out with values of gains computed using the classical technique for second order systems, that is to say from requirements of a damping ratio around 0.7 and a settling time.

This campaign led to mixed results, which are not presented here, where the depth of discharge could change very strongly from 16 to almost 30% for very limited variations of Kp and Kd. It was moreover impossible to extract any kind of trend linking the evolution of the gains with that of the DoD.

By expanding the range of values admitted for Kd to reach significantly higher damping ratios, it could be seen that the system behaved much more predictably with respect to gains variations.

For the 2-axis controller with momentum monitoring (Ks=0), results degraded significantly when the damping ratio fell under 2. The link between the performance and damping ratio is particularly important for the pointing accuracy, as can be seen in Figure 9 (The direction of increasing damping ratio is from top left to bottom right). Concerning convergence time and DoD, the results are less dependent upon the value of the damping ratio as long as it is higher than 2 (Figure 7).

Trying to control the angular rate of the Z-axis substantially degrades the performances for all criteria as can be seen by comparing Figure 7 to Figure 8, and Figure 9 to Figure 10. This result was expected since the physical limitations of magnetic actuation only allow to control 2 axes at a time.

Although the 3-axis controller with kinetic momentum has the best performances regarding DOD and convergence time, it is the 2-Axis controller that performs best for pointing accuracy. The evolution of the depointing error for the best controller of each strategy are presented in Figure 11 and Figure 12. Their respective parameters and performances are summarized in Table 2 and Table 3.

The results for both controllers satisfy the 30° criterion, but the accuracy of the 2-axis controller is particularly striking. Another striking feature that can be observed in Figure 11 is the attitude stability during eclipses, although the controller is then turned off. This behaviour marks the presence of a stabilizing spin around the pointed axis. It could seem difficult to understand, as no spin is ever commander about that axis. It can actually be explained by the way the commanded torques are transformed into requested magnetic moment. Indeed, the process considers the torques as being in the plane normal to the magnetic field. But if they are not, it can be shown that when "translated" into magnetic moment, the components of the commanded torque will spill over all the axes, including Z, and therefore induce a spin.

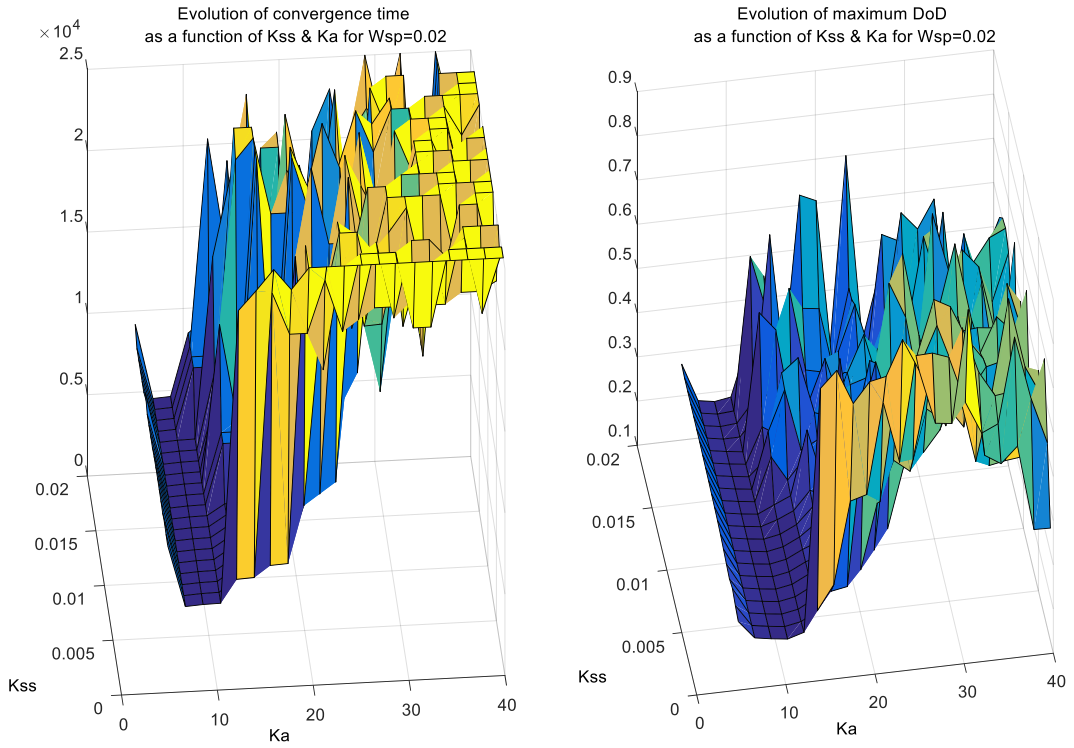

Figure 5: Evolution of convergence time and DOD as a function of the gains for Wsp=0.02 (3-axis control with kinetic momentum)

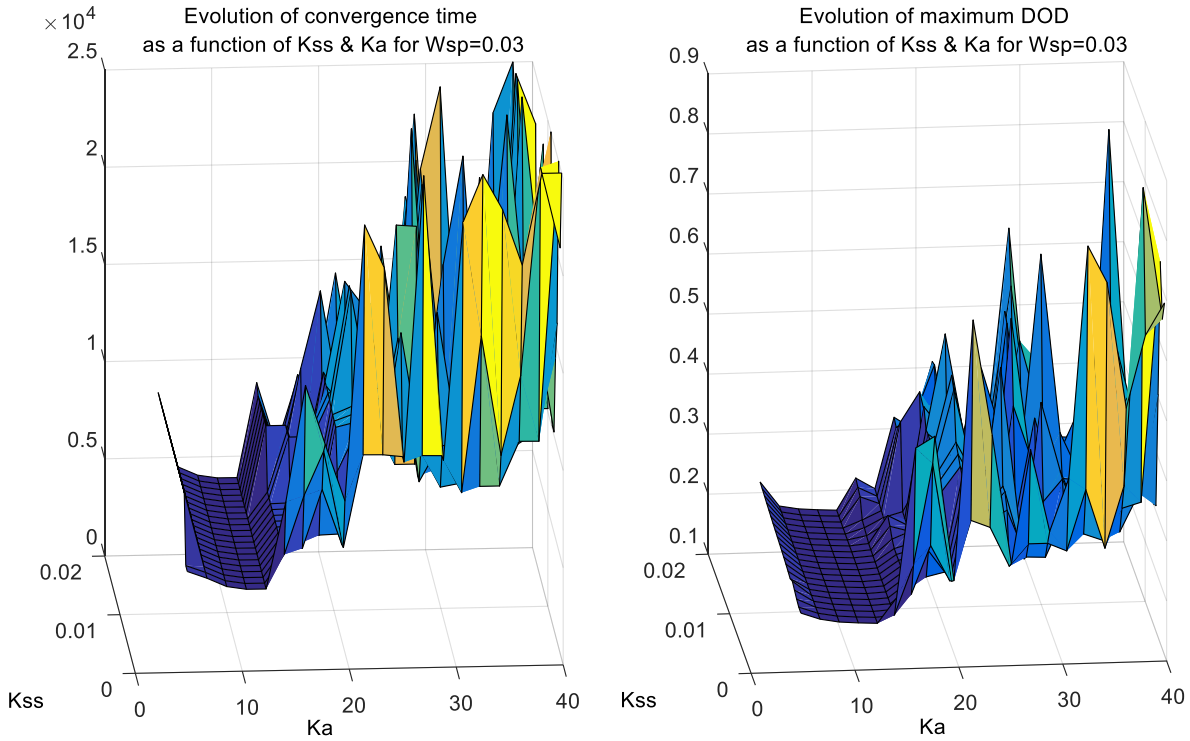

Figure 6: Evolution of convergence time and DOD as a function of the gains for Wsp=0.03 (3-axis control with kinetic momentum)

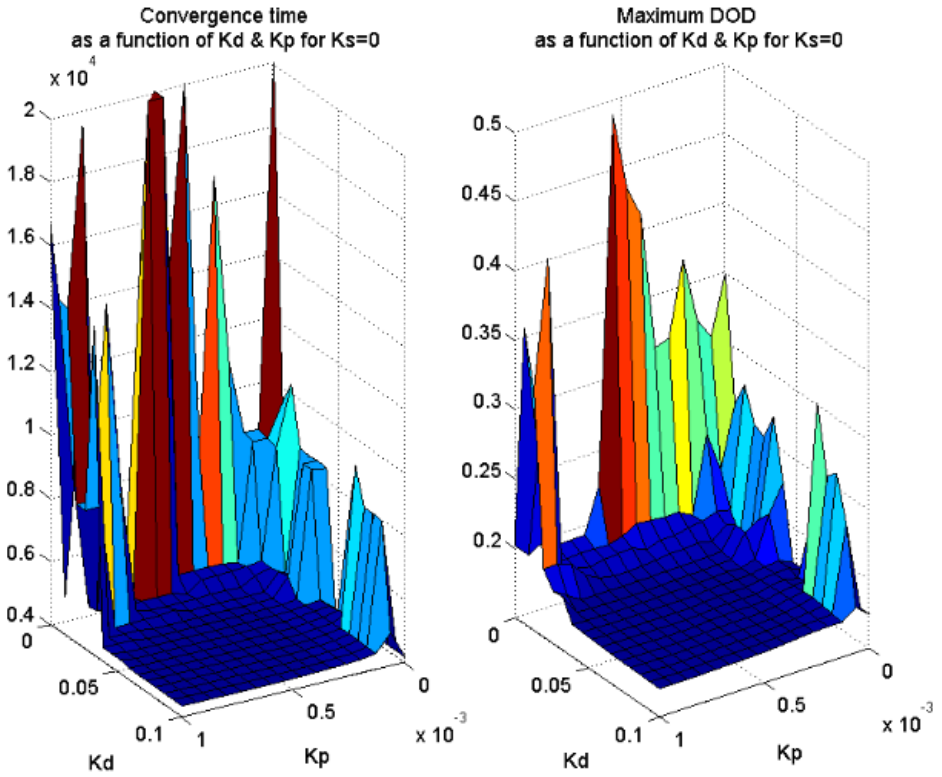

Figure 7: Evolution of convergence time and DOD as a function of Kp and Kd for $K_s = 0$ (2-axis control with kinetic momentum monitoring)

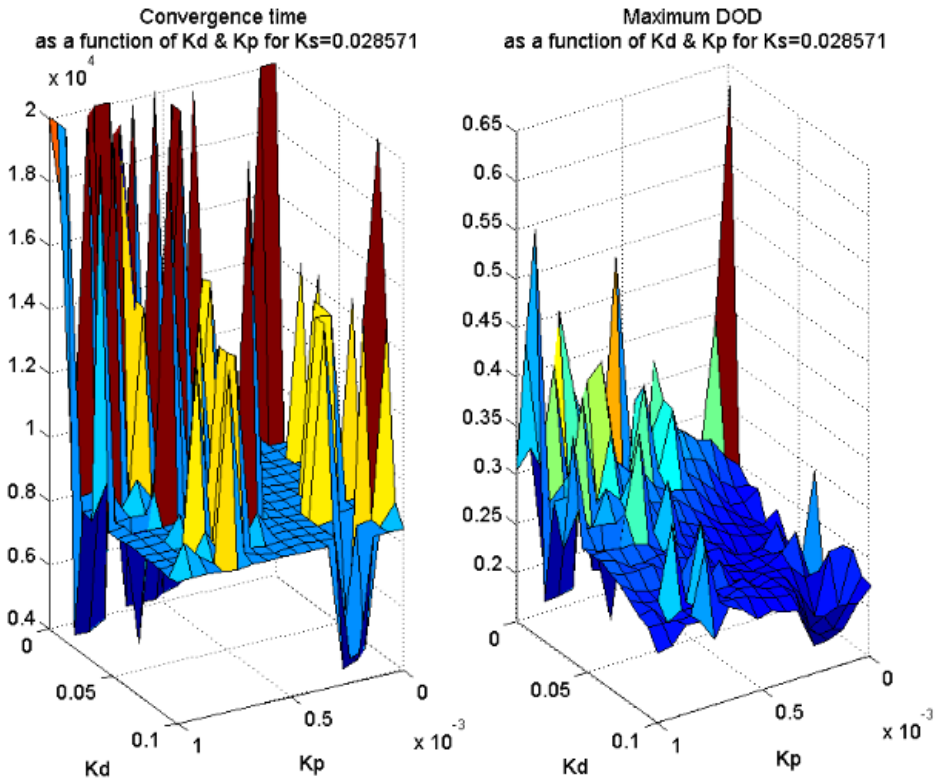

Figure 8: Evolution of convergence time and DOD as a function of Kp and Kd for $K_s \neq 0$ (3-axis control without kinetic momentum)

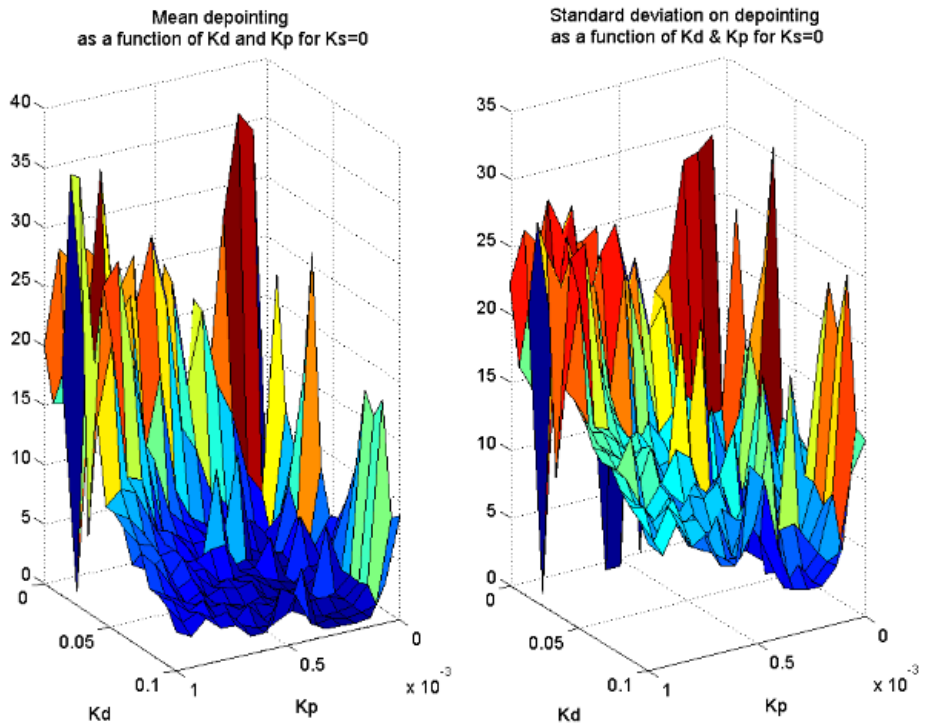

Figure 9: Evolution of mean depointing and standard deviation as a function of Kp and Kd for $K_s = 0$ (2-axis control with kinetic momentum monitoring)

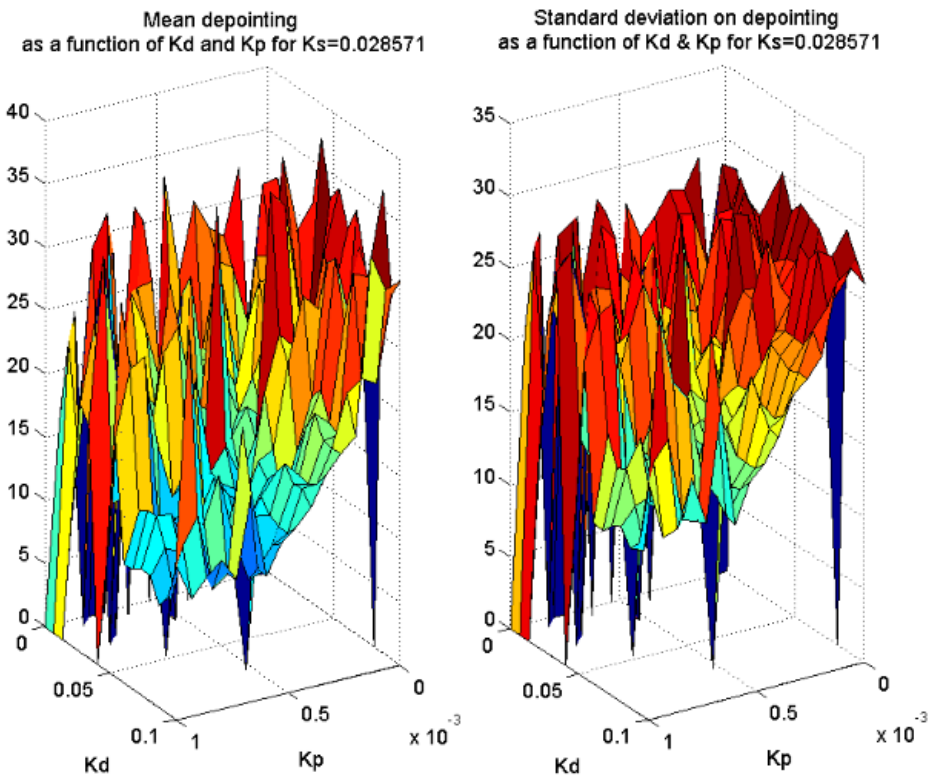

Figure 10: Evolution of mean depointing and standard deviation as a function of Kp and Kd for $K_s \neq 0$ (3-axis control without kinetic momentum)

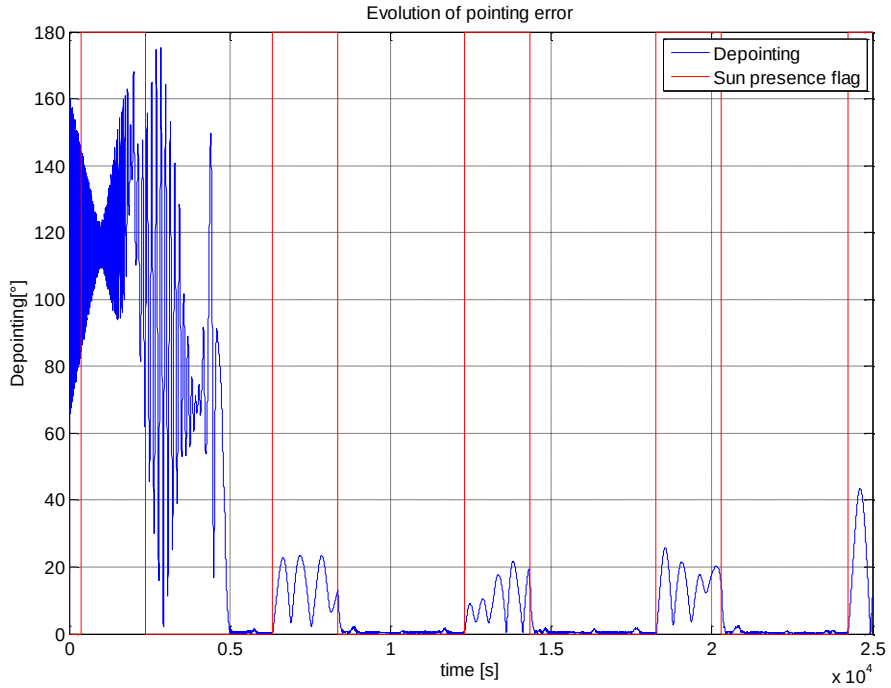

Figure 11: Evolution of depointing error
(Best result 2-axis control with kinetic momentum monitoring)

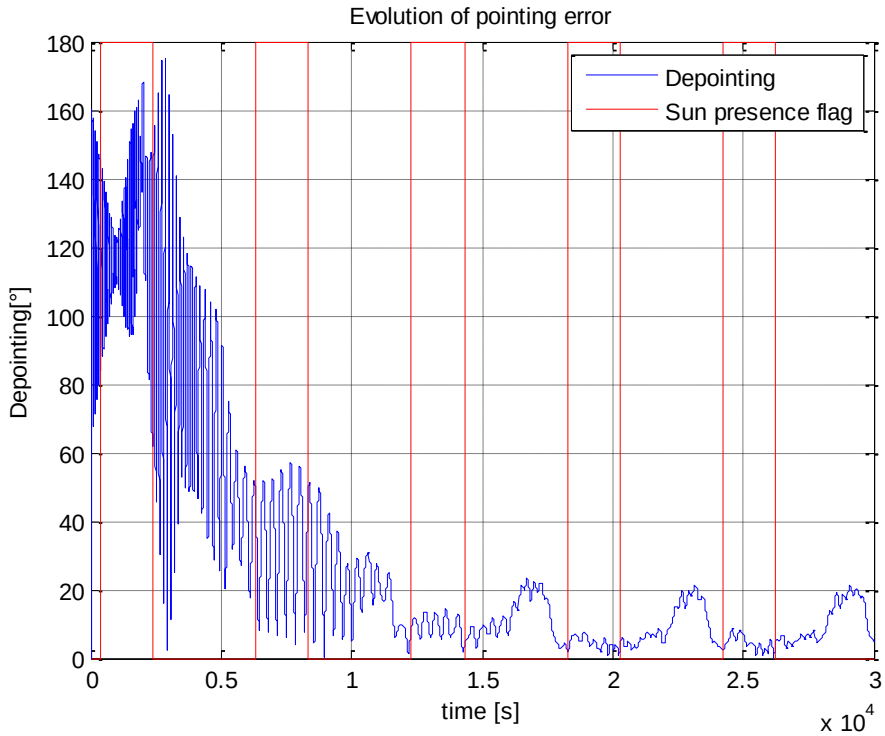

Figure 12: Evolution of depointing error
(3-axis control without kinetic momentum)

Table 2: Best parameters and performances for 2-Axis Controller

2-Axis controller with momentum monitoring	
Parameter	**Value**
Kp [/]	0.00065
Kd [/]	0.013571
Convergence time [s]	4760
Maximum DoD [%]	18.35
Mean error angle after convergence [°]	0.44
Standard deviation angle after convergence [°]	1.11

Table 3: Best parameters and performances for 3-axis controller with kinetic momentum

3-axis controller with kinetic momentum	
Parameter	**Value**
Ka [/]	13.3729
Ks [/]	0.0019474
Wspin [rad/s]	0.03
Convergence time [s]	4511.75
Maximum DoD [%]	17.7
Mean error angle after conv. [°]	10.5885

CONCLUSION

In this work, 3 candidate strategies for the attitude control in safe mode have been evaluated. Each strategy could be modelled theoretically, and criteria for stability and parameters selection have been determined in each case.

The 3 controllers have been be implemented in the simulation environment of CNES, and their performances compared in terms of pointing accuracy and convergence time. This comparative study revealed that the best strategy to obtain a good pointing accuracy is the 2-axis position controller with kinetic momentum monitoring. The addition of a speed control gain in the 3-axis position controller without kinetic momentum only degrades the performances and increases consumption.

Concerning the convergence time and maximum DOD, the best strategy seems to be the 3-axis controller with kinetic momentum. The pointing accuracy is in that case a bit poorer, but the gain in convergence time and power gives it the advantage for a safe mode.

The study also allowed confirming the theoretical results, in particular the ranges obtained for the gains.

As a control strategy meeting the pointing and convergence time requirements could be found, it can be said that the objective has been met.

In the future, this work could be extended by a robustness analysis of the 3 strategies with respect to uncertainties such as variations in the inertia matrix or residual magnetic moment. It could also be interesting to study in more detail the unintended spin that appears in the 2 axis control strategy. This behaviour does not threaten stability when it is handled properly, but its understanding could provide more insight on the internal dynamic of this control method.

REFERENCES

1. **Ressouche, A., Apper, F. and Gaboriaud, A.** *EyeSat: A Student Triple Cubesat for Astronomy.* Valletta (Malta) : 4S Symposium, 2016.

2. **Viaud, F. and Lagrange, O.** *Safe Mode Attitude Control of EyeSat Mission.* Warsaw (Poland) : EuroGNC, 2017.

3. **Sidi, Marcel J.** *Spacecraft dynamics and control.* Cambridge, UK : Cambridge university press, 1997.

4. **Wertz, James R.** *Spacecraft attitude determination and control.* Dordrecht : D. Riedel Publishing Company, 1978.

5. **Le Du, M., J., Maureau and Prieur, P.** *Myriade, an adaptative concept.* Frascati : 4th GNC ESA, 2002.

6. **Steyn, W.H. and Hashida, Y.** *In-Orbit Attitude and Orbit Control Commissioning of UoSAT-12.* GuildFord, GU2 5XH : Surrey Space Centre, University of Surrey, 2000.